GAS-PHASE MIXING IN BUBBLE COLUMNS

MIKIO KAWAGOE
Department of Chemical Engineering, Nara National College of Technology, Yamato-Koriyama 639–11
TSUTAO OTAKE
Department of Industrial Chemistry, Chubu University, Kasugai 487
CAMPBELL W. ROBINSON
Department of Chemical Engineering, University of Waterloo, Waterloo, Ontario, Canada N2L 3G1

Key Words: Mixing, Bubble Column, Reactor, Residence Time Distribution, Axial Dispersion Coefficient

Residence time distributions of gas phase in bubble columns were obtained by excluding end effects from observed responses to pulse inputs of tracer, using Fourier transforms. Based on the behavior of the residence time distributions, a gas-phase mixing model was proposed in which bubble swarm was assumed to be composed of two bubble groups, one in the core (or central) region and the other in the annular (or peripheral) region of the column. As a result, it was found that about 80 % of all the bubbles are rising in the core region and that gas-phase mixing is more intensive in the core region than in the annular region. Axial dispersion coefficients in each bubble group were correlated empirically.

Introduction

Bubble columns are widely used in the chemical and biochemical industries. Although it is known that gas-phase mixing as well as liquid-phase mixing is a significant factor in the design and scale-up of bubble columns,[2] gas-phase mixing has not been studied as extensively as liquid-phase mixing. The main reason for this is the difficulty in measuring the residence time distribution (RTD) of bubbles because of the time delay in the detector when measuring tracer concentration and the large end effect in the gas-liquid disengagement section at the top of the bubble column.

In most past investigations, a one-dimensional axial dispersion model has been applied to gas-phase mixing to determine the gas-phase axial dispersion coefficient.[1,3,4,8,9,11] On the other hand, Molerus *et al.*[7] pointed out that the applicability of the one-dimensional dispersion model to gas-phase mixing is questionable because of the great inhomogeneity in behavior of bubbles due to intensive turbulent liquid

Received June 6, 1988. Correspondence concerning this article should be addressed to M. Kawagoe.

recirculation flow in the bubble column. Such flow has been observed under certain conditions, and a theory of recirculation flow was provided by Ueyama *et al.*[12)]

In the present work to investigate gas-phase mixing in bubble columns, first the RTD in the gas-liquid dispersion section alone was computed, using Fourier transforms. Then a model of gas-phase mixing was proposed, reflecting the behavior of the RTD obtained. Based on the model, the influence of gas velocity, column diameter and liquid system on gas-phase mixing was investigated experimentally.

1. Analytical Method

As shown in **Fig. 1**, the measurement system can be divided into three sections: the gas introduction section, gas-liquid dispersion section, and gas-liquid disengagement section. As will be discussed below, since the tube arrangement was designed so that the flow of gas in the gas introduction section from the tracer injection point to the gas sparger at the bottom of the column could be assumed to be plug flow, the overall RTD in the measurement system as a whole was corrected by subtracting the time lag in this section. Since the overall RTD, $E_O(t)$, is a convolution of RTD in the gas-liquid dispersion section, $E(t)$, and RTD in the gas-liquid disengagement section including the detector, $E_T(t)$, the following relation holds among these three RTDs.[6)]

$$E_O(t)=\int_0^t E(t_o)E_T(t-t_o)dt_o \qquad (1)$$

Hence, the unknown $E(t)$ is obtained by deconvolution. It was carried out by Fourier transforms as follows.

$$e_O(\omega)=\int_{-\infty}^{\infty} \exp(-2\pi i\omega t)E_O(t)dt \qquad (2)$$

where $e_O(\omega)$ is an image function of $E_O(t)$ by Fourier transform. From Eqs. (1) and (2), the following equation was obtained.

$$e_O(\omega)=e(\omega)e_T(\omega) \qquad (3)$$

where $e(\omega)$ and $e_T(\omega)$ are the image functions of $E(t)$ and $E_T(t)$, respectively. Then $e(\omega)=e_O(\omega)/e_T(\omega)$. Thus the $E(t)$ desired can be evaluated by inverse Fourier transform as follows.

$$E(t)=\frac{1}{2\pi}\int_{-\infty}^{\infty} \exp(2\pi i\omega t)e(\omega)d\omega \qquad (4)$$

Calculations were carried out by fast Fourier transform (FFT), because data were obtained as discrete variables.

2. Experimental

A schematic diagram of the experimental equipment is shown in **Fig. 2**. Two bubble columns, column I of 0.159 m diameter and column II of 0.290 m diameter, were used. The gas-liquid dispersion height in both columns was maintained at 2 m. Column I and column II were made of glass and transparent acrylic resin, respectively. Perforated plates with holes of 2 mm diameter were used as gas spargers. For column I the perforated plate has 2 mm thickness and 61 holes (free area 0.97%), and for column II it has 5 mm thickness and 198 holes (free area 0.94%). The perforated plate was made of stainless steel for the column I and acrylic resin for column II, respectively. To reduce the effect on the RTD of gas-phase mixing in the section under the perforated plate, the height of the section was taken to be as small as 5 mm. The clearance of 5 mm under the plate was high enough for homogeneous bubbling on the plate. Accordingly, the effect of radial distribution of tracer concentration was neglected.

Gas-phase mixing was measured by pulse response method. Helium gas was used as tracer. First, to measure the RTD in total measurement system, $E_O(t)$, an amount of tracer of 91 cm³ was injected into the gas stream entering at the bottom of the column. The

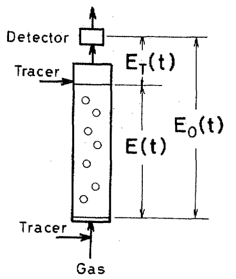

Fig. 1. Measurement system

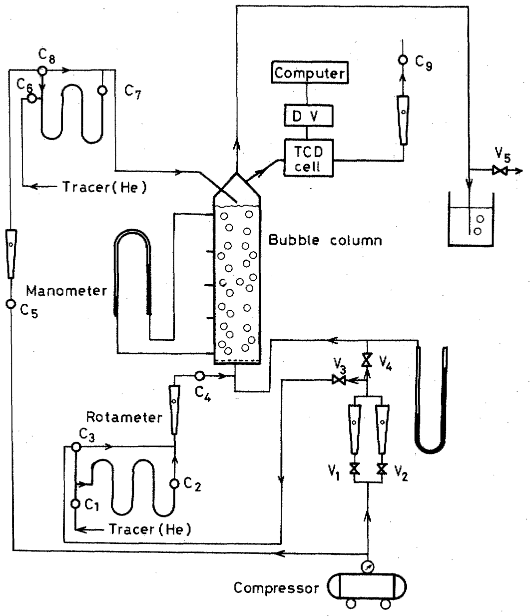

Fig. 2. Experimental equipment

concentration of the tracer in the gas stream leaving the column was measured at the top of the column by a thermal conductivity detecor (TCD). Data were taken into a microcomputer (NEC PC-8801) with a sampling speed of 2.44 s^{-1} through a digital voltmeter (DV) connected to the TCD. To suppress the disturbance of gas flow rate caused by tracer injection, carrier gas was branched from the main flow of gas. The tracer filled in a chamber in advance was injected by changing flow pass of the carrier gas by operating the cocks shown in Fig. 2. Then, to obtain the RTD in the gas-liquid disengagement section and the detecor, $E_T(t)$, the same measurement was carried out, injecting tracer into the top section of the column. To prevent the mixing in the carrier gas line, thin glass tube of 6 mm inside diameter was used for the line.

All of the experiments were carried out by employing air and batch liquid. The liquid used were tap water, sodium sulfate aqueous solution (1/3 kmol/m^3) and carboxymethyl cellulose (CMC) aqueous solution (0.5 wt.%). The CMC solution has been employed as model fluid of culture. The apparent viscosity of the CMC solution measured by the rotational viscometer was about 30 mPa·s. Since the concentration of CMC is low, deviation in property from the Newtonian fluid is considered to be small.

Mean gas holdup was determined from axial distribution of static pressure measured at the wall of the column.

3. Results and Discussion

3.1 Gas holdup and flow regime in bubble columns

Plots of gas holdup, $\bar{\varepsilon}_G$, versus superficial gas velocity, u_G are shown in **Fig. 3**. In general, flow regime in the bubble column is bubbly flow at low gas velocities, and turbulent recirculation flow at high gas velocities. Sakata *et al.*[10] characterized the flow regime using an empirical correlation for gas holdup given by Kato *et al.*,[5] which consists with the gas holdup in the turburent recirculation flow regime. They found that for perforated plates with holes having diameter greater than 2 mm, no bubbly flow exist and turbulent recirculation flow prevails even at low gas velocities. As can be seen from Fig. 3, gas holdups in this experiment agree well with the correlation by Kato *et al.*, except for CMC system in column I. This implies that the flow regime is the turbulent recirculation flow throughout the entire range of gas velocity in this experiment. For CMC system in column I, bubble slugs were observed. This is the reason for the smaller gas holdup in column I for CMC system than for the other cases.

3.2 Residence time distribution

An example of $E_O(t)$ and $E_T(t)$, together with $E(t)$ computed by FFT, are shown in **Fig. 4**. Behavior of the $E(t)$ was found to be complicate, compared to the

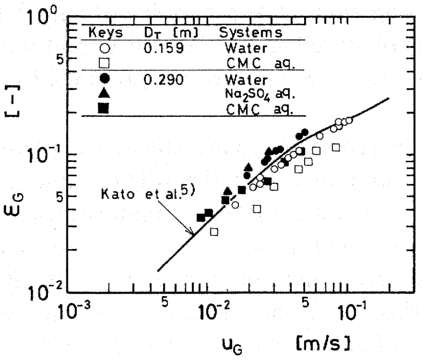

Fig. 3. Gas holdup, $\bar{\varepsilon}_G$, as a function of superficial gas velocity, u_G

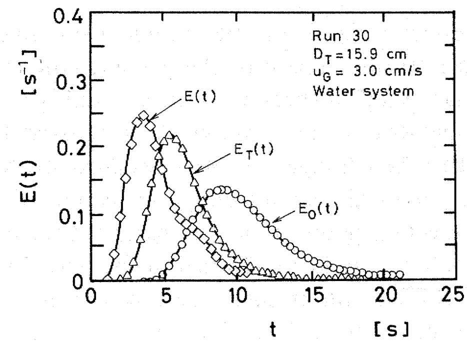

Fig. 4. Example of residence time distribution in each section of bubble column

monotonous variation of the $E_O(t)$.

In **Fig. 5**, RTD curves under various conditions are plotted against nondimensional time, $\theta(=t/\tau)$, where τ is the mean residence time calculated from the first moment. The mean residence time can also be estimated as $\bar{\varepsilon}_G H_T/u_G$, dividing the total dispersion height, H_T, by average bubble rising velocity, $u_G/\bar{\varepsilon}_G$. The mean residence times deduced from these two methods agree with each other within an error of $\pm 15\%$.

1) Influence of gas velocity Figure 5-(a) depicts RTD curves for two different gas velocities. These plots show that the peak of RTD becomes low and its width broadens as the gas velocity increases.

2) Influence of column diameter Influence of column diameter on RTD can be seen from the comparison of the RTDs of Run 30 and Run 120 shown in Fig. 5-(b). The peak of RTD is lower and its width is broader for large column diameter than those for small column diameter.

3) Influence of system For column I, influence of liquid system on RTD can be seen in Fig. 5-(b). The RTD for CMC system (Run 63) has higher peak and narrower width than the one for water system (Run 30). The value of θ at which RTD takes maximum value is nearer to unity for the CMC system than that for the water system.

RTD for column II is displayed in Fig. 5-(c). Not so much difference in behavior of RTD is observed

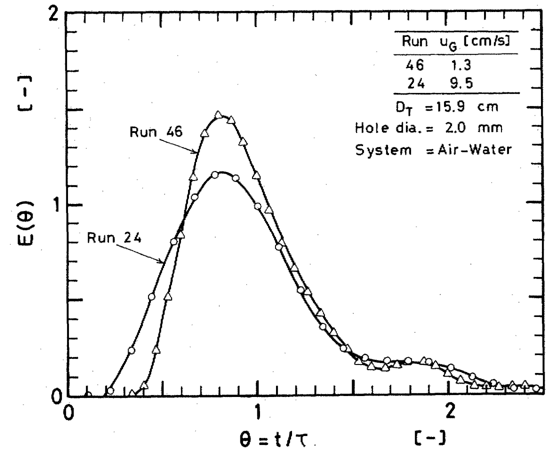

(a) Influence of u_G on RTD

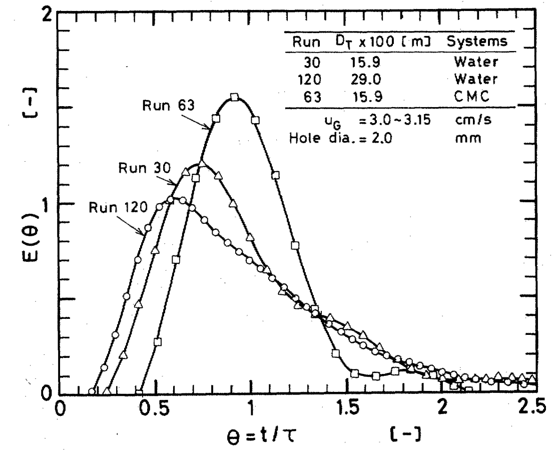

(b) Influence of column diameter and liquid system on RTD

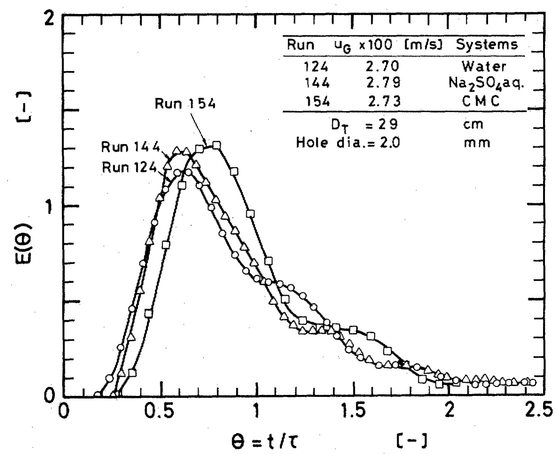

(c) Influence of liquid system on RTD for column II

Fig. 5. Residence time distribution (RTD) under various conditions

between the water system (Run 124) and the sodium sulfate system (Run 144). Also, difference in behavior of RTD between the water and the CMC systems is small for column II, compared to that for column I.

For any case mentioned above, the RTD has a "hump" in the course of decrease after taking a maximum, which means that bubble swarm in the column consists of not a single bubble group but two or more bubble groups. This fact suggests that the gas-phase mixing would not be expressed by such a simple model as the dispersion model used in the past investigations.[1,3,4,8,9,11]

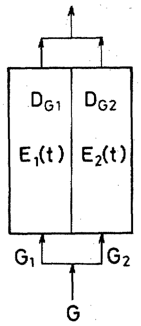

Fig. 6. Gas-phase mixing model

3.3 Mixing model

In the bubble column, there exists a liquid circulation flow, that is, upflow in the core region and downflow near the wall of the column.[12] In the upflow region, since larger bubbles with higher ascending velocity pass through, the bubble group has shorter mean residence time than that in the downflow region.

As show in **Fig. 6**, two bubble groups are assumed, which are the bubble group 1 in the upflow region and the bubble group 2 in the downflow region near the wall of the column. For simplification, we assume no exchange of bubbles between the two groups. Neglecting interphase mass transfer of the tracer according to Field *et al.*[4] and Van Vuuren,[14] mass balance on the tracer in each bubble group gives the following equation.

$$\frac{\partial C_i}{\partial t} = D_{Gi}\frac{\partial^2 C_i}{\partial z^2} - \frac{u_{Gi}}{\overline{\varepsilon_{Gi}}} \cdot \frac{\partial C_i}{\partial z} \tag{5}$$

where D_{Gi} is the gas phase dispersion coefficient, C_i the tracer concentration, and $\overline{\varepsilon_{Gi}}$ the mean gas holdup in each bubble group. The subscript, i, designates the bubble group: $i=1$ for group 1 and $i=2$ for group 2. The solution of Eq. (5) gives the RTDs in each bubble group, $E_1(t)$ and $E_2(t)$ (see **Appendix A**). Since $E(t)$ is the resultant RTD of $E_1(t)$ and $E_2(t)$, the following relationship holds.

$$E(t) = \alpha E_1(t) + (1-\alpha)E_2(t) \tag{6}$$

where $\alpha = G_1/G$: G_1 is the gas flow rate in bubble group 1, and G the total gas flow rate. The gas holdup $\overline{\varepsilon_{Gi}}$ and the gas velocity u_{Gi} in each bubble group can be estimated from the radial distribution of gas holdup in the bubble column (see **Appendix B**). Therefore, Eq. (6) has three unknown parameters, α, D_{G1} and D_{G2}. In the present work, the unknown parameters were determined by the method of least squares. **Figure 7** shows a comparison of the observed RTDs with the values calculated from Eq. (6). In Fig. 7, estimation by the conventional dispersion model used in past investigations is depicted by a broken line, in which the dispersion coefficient was determined by the method of least squares. As can be seen from Fig. 7, agreement is much better for the present model than for the conventional dispersion model. The α, D_{G1} and D_{G2} obtained are discussed below.

1) Fraction of gas flow rate in upflow region, α **Figure 8** shows plots of $\alpha/(1-\alpha)$ versus u_G. It was found that most $\alpha/(1-\alpha)$ take values from 3 to 5 in the range of u_G less than 0.05 m/s, except for the CMC system in column I. Thus, $\alpha/(1-\alpha)$ is taken to be approximately 4; that is, α is nearly equal to 0.8. At high gas velocities, the turbulence in the bubble column becomes violent, causing an exchange of bubbles between the two bubble groups. The sudden drop of $\alpha/(1-\alpha)$ for $u_G > 0.08$ m/s is considered to be due to this vigorous exchange of bubbles.

For the CMC system, as the flow regime is slug flow in column I, the value of α, which is approximately 0.71, is smaller than that in the other case mentioned above. For column II, since the column diameter is large, slug flow is hardly attained even for the CMC system, so that α takes values close to those for the water system.

2) Dispersion coefficients Taking into account the results in past investigations,[4,8,9] the dominant factors for gas-phase mixing are mean ascending velocity of bubbles $u_G/\overline{\varepsilon_G}$ and column diameter D_T. Plots of the dispersion coefficients versus $u_G/\overline{\varepsilon_G}$ with a parameter of D_T are shown in **Fig. 9**. It was found from the plots that the values of D_{G1} in the upflow region are about three times larger than those of D_{G2} in the downflow region, which indicates that gas-phase mixing is more intensive in the upflow region than in the downflow region.

First, we discuss the dispersion coefficients for the water and sodium sulfate solution systems. The plots in Fig. 9 reveal that the dispersion coefficients, D_{G1} and D_{G2}, may be correlated by straight lines depending on the column diameter, D_T. From the plots shown in Fig. 9-(a), the following equation was obtained.

$$D_{G1}=26.2\left[\frac{u_G}{\overline{\varepsilon_G}}\right]^{3.03}(D_T)^{1.79} \tag{7}$$

Also, plots for D_{G2} displayed in Fig. 9-(b) give the following equation.

$$D_{G2}=19.4\left[\frac{u_G}{\overline{\varepsilon_G}}\right]^{3.4}(D_T)^{2.1} \tag{8}$$

Although gas holdup in the sodium sulfate solution system was slightly larger than that in the water system due to small bubbles formed by breakup, there is no definite difference in the values of D_{G1} and D_{G2} between the two systems. It seems that gas-phase mixing is little affected by small bubbles.

Next, we discuss whether the correlations obtained above can be applied to the CMC system. Comparison of the dispersion coefficients observed for the CMC system with Eqs. (7) and (8) is shown in **Fig. 10**. From the comparison, it was found that the

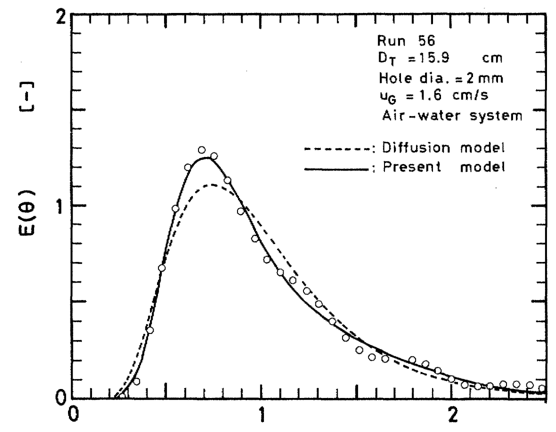

Fig. 7. Comparison of residence time distributions observed with those calculated by present model and by conventional diffusion model

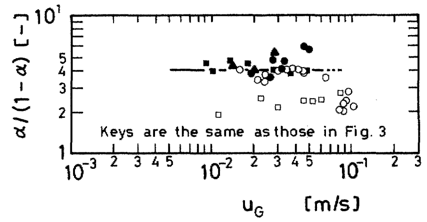

Fig. 8. Relation between $\alpha/(1-\alpha)$ and u_G

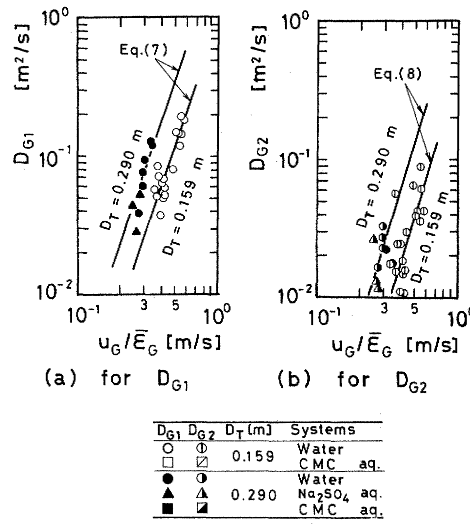

Fig. 9. Correlation of D_{G1} and D_{G2} as a function of $u_G/\overline{\varepsilon}_G$ with parameter of D_T for water and sodium sulfate solution systems

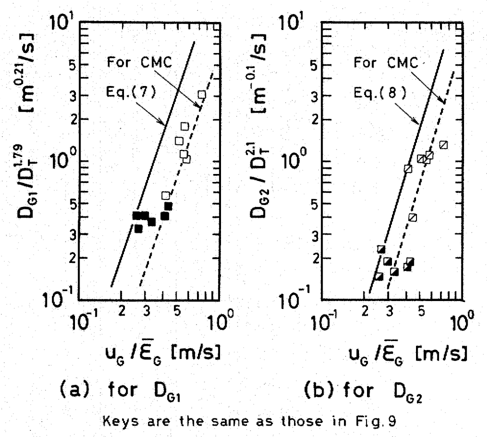

Fig. 10. Comparison of D_{G1} and D_{G2} for CMC system with Eqs. (7) and (8)

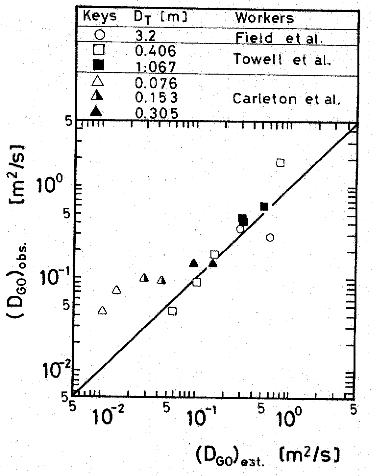

Fig. 11. Comparison of D_{GO} estimated from the present model with values observed in past investigations

values of D_{G1} and D_{G2} for the CMC system are smaller than Eqs. (7) and (8). For column I, the observed values are one-quarter to one-half those for the water system. Hence, for the slug flow regime we may replace the constant 26.2 in Eq. (7) with 6.3, and the constant 19.4 in Eq. (8) with 7.4, which are displayed by broken lines in Fig. 10.

On the other hand, for column II theD_{G1} and D_{G2} take value close to those of the water system at low values of $u_G/\bar{\varepsilon}_G$. At high gas velocities, slug flow was not observed but bubbles coalesced to large ones, and the values of D_{G1} and D_{G2} were close to those of slug flow. For large columns as in this work, large bubbles seem to decrease the values of D_{G1} and D_{G2}, even if slug flow is not realized.

Consequently, the correlations obtained above can be applied to the water system and systems similar to water. To obtain the general correlations of gas-phase mixing, it is necessary to investigate further the effect of liquid properties.

3.4 Comparison with previous investigations

To obtain a relationship between variance of the total system, σ_O^2, and variances of the two groups, σ_1^2 and σ_2^2, both sides of Eq. (6) are multiplied by $(t-\tau)^2$ and then integrated from zero to infinite. The relationship is given by the following equation.

$$\sigma_O^2=\alpha\sigma_1^2+(1-\alpha)\sigma_2^2+\alpha(1-\alpha)(\tau_1-\tau_2)^2 \qquad (9)$$

In general, for a closed system the following relationship holds between σ_O^2 and Pe_O.[13]

$$\sigma_O^2/\tau^2=(2/Pe_O^2)\{Pe_O-1+\exp(-Pe_O)\} \qquad (10)$$

If $Pe_O \geqq 10$, the above expression may be approximated by $\sigma_O^2/\tau^2=2/Pe_O$ within an error of 11%. The same also holds for σ_1^2 and σ_2^2. In most past investigations,[1,3,4] the dispersion coefficient, which is designated by D_{GO}, was estimated from Eq. (10), assuming that the bubble swarm in the bubble column is composed of a single bubble group. Therefore, the relationship between D_{GO} in past works and D_{G1} and D_{G2} in the present work is given by substituting Eq. (10) for σ_O^2 and the same relations for σ_1^2 and σ_2^2 into Eq. (9). For simplification, $\alpha=0.8$ and $\phi_C=\sqrt{2}/2$ (see Appendix B) were taken, according to the result of the present work. Since the values of the Peclet number in the present work are greater than 10, the following equation was obtained.

$$D_{GO}=0.66D_{G1}+0.39D_{G2}+0.0078(u_G H_T/\bar{\varepsilon}_G) \qquad (11)$$

If $D_T \geqq 0.1$ m and $H_T/D_T \leqq 20$, the third term on the right-hand side can be neglected, since the contribution of the third term is less than 10%. Results of D_{GO} in the past investigations[1,4,11] estimated from Eqs. (7), (8) and (11) are shown in **Fig. 11**. It was found that the estimated values agree approximately with the data.

Conclusions

Residence time distribution of gas in gas-liquid dispersion alone was computed, by employing Fourier transforms. To describe the residence time distributions obtained, a gas-phase mixing model was presented, in which two bubble groups, one in the core region and the other in the annular region, were assumed. Applying the dispersion model to each bubble group, the fraction of gas flow rate and dispersion coefficients in each bubble group were calculated.

It was found that the fraction of gas flow rate passing through the core region to total gas flow rate is about 80%, and that gas-phase mixing is more intensive in the core region than in the annular region. Also, dispersion coefficients estimated from the correlations proposed agree with those obtained past investigations.

Appendix A

From the solution of Eq. (5) for a closed system,[15] the residence time distribution is given as follows.

$$\tau_i E_i(t) = 2\exp\{(Pe_i/2)(1 - t/2\tau_i)\}$$
$$\times \sum_{n=1}^{\infty} \frac{4(-1)^{n+1}\delta_n^2}{4Pe_i + Pe_i^2 + 4\delta_n^2} \exp(-\delta_n^2 t/Pe_i\tau_i) \quad \text{(A-1)}$$

where $Pe_i = u_{Gi}H_T/\overline{\varepsilon_{Gi}}D_{Gi}$, $\tau_i(=\overline{\varepsilon_{Gi}}H_T/u_{Gi})$, and δ_n is the n-th positive root of the following equation.

$$\tan\delta_n = \frac{4Pe_i\delta_n}{4\delta_n^2 - Pe_i^2} \quad \text{(A-2)}$$

Appendix B

The lateral distribution of gas holdup has been given as follows.[12]

$$\varepsilon_G = \frac{n+2}{n}\overline{\varepsilon_G}(1-\phi^n) \quad \text{(B-1)}$$

where $\phi = r/R$; r is radial coordinate from the center and R is radius of the column. If the radial coordinate of the point at which the time-averaged local liquid velocity is zero is designated by r_C, the region where $r < r_C$ is the upflow region, and the region where $r_C < r < R$ is the downflow region. Hence, bubbles in the region of $r < r_C$ and those in the region of $r_C < r < R$ are defined as bubble group 1 and bubble group 2 respectively. Since the value of n is taken to be 2,[12] the mean gas holdups in the upflow and the downflow regions, $\overline{\varepsilon_{G1}}$ and $\overline{\varepsilon_{G2}}$, are expressed by the following equation.

$$\overline{\varepsilon_{G1}} = \overline{\varepsilon_G}(2-\phi_C^2) \quad \text{(B-2)}$$

$$\overline{\varepsilon_{G2}} = \overline{\varepsilon_G}(1-\phi_C^2) \quad \text{(B-3)}$$

where the value of $\phi_C(=r_C/R)$ can be estimated from the liquid recirculation model presented by Ueyama et al.[12] Since the variation in ϕ_C with operating variables and column diameter is small, $\phi_C = \sqrt{2}/2 = 0.7$, which is the value for the case where mean velocities of liquid in the upflow region and the downflow region are equal to each other, may be used approximately for batch liquid.

The superificial gas velocities in the upflow and the downflow regions, u_{G1} and u_{G2}, are given as follows.

$$u_{G1} = G_1/\pi r_C^2 = \alpha u_G/\phi_C^2 \quad \text{(B-4)}$$

$$u_{G2} = G_2/\pi(R^2 - r_C^2) = (1-\alpha)u_G/(1-\phi_C^2) \quad \text{(B-5)}$$

Nomenclature

C	= tracer concentration	[kmol/m^3]
D_G	= gas-phase dispersion coefficient	[m^2/s]
D_T	= column diameter	[m]
$E(t)$	= residence time distribution	[s^{-1}]
$E(\theta)$	= $\tau E(t)$, nondimensional residence time distribution	[—]
$e(\omega)$	= image function of $E(t)$ by Fourier transform	[—]
G	= gas flow rate	[m^3/s]
H_T	= column height	[m]
Pe	= $u_G H_T/\overline{\varepsilon_G} D_G$, Peclet number	[—]
R	= radius of column	[m]
r	= radial coordinate	[m]
t	= time	[s]
u_G	= superficial gas velocity	[m/s]
α	= G_1/G, fraction of gas flow rate of bubble group 1 to total gas flow rate	[—]
$\overline{\varepsilon_G}$	= mean gas holdup	[—]
θ	= t/τ, nondimensional time	[—]
σ	= standard deviation	[s]
τ	= mean residence time	[s]
ϕ	= r/R, nondimensional radial coordinate	[—]
ω	= variable used in Fourier transform	[s^{-1}]

⟨Subscripts⟩

1	= bubble group 1
2	= bubble group 2
C	= position at which time-averaged local liquid velocity is zero
O	= overall
T	= top

Literature Cited

1) Carleton, A. J., R. J. Flain, J. Rennie and F. H. H. Valentin: *Chem. Eng. Sci.*, **22**, 1839 (1967).
2) Deckwer, W.-D.: *Int. Chem. Eng.*, **19**, 21 (1979).
3) Diboun, M. and K. Schügerl: *Chem. Eng. Sci.*, **22**, 147 (1967).
4) Field, R. W. and J. F. Davidson: *Trans. Instn. Chem. Engrs.*, **58**, 228 (1980).
5) Kato, Y. and A. Nishiwaki: *Kagaku Kōgaku*, **35**, 912 (1971).
6) Levenspiel, O.: "Chemical Reaction Engineering," 2nd Ed., John Wiley & Sons, Inc., p. 263 (1972).
7) Molerus, O. and M. Kurtin: *Chem. Eng. Sci.*, **41**, 2693 (1986).
8) Mangartz, K. H. and Th. Pilhofer: *Verfahrenstechnik*, **14**, 40 (1980).
9) Pilhofer, Th., H. F. Bach and K. H. Mangartz: 5th Int. Sympos Chemical Reaction Engineering, 31 ACS, Washington D.C. (1978).
10) Sakata, M. and T. Miyauchi: *Kagaku Kogaku Ronbunshu*, **6**, 428 (1980).
11) Towell, G. D. and G. H. Ackermann: Proc. 5th Europ. 2nd Int. Symps. Chemical Reaction Engineering B3-1, Elsevier, Amsterdam (1972).
12) Ueyama, K. and T. Miyauchi: *AIChE J.*, **25**, 258 (1979).
13) Van der Laan, E. T.: *Chem. Eng. Sci.*, **7**, 187 (1958).
14) Van Vuuren, D. S.: *Chem. Eng. Sci.*, **43**, 213 (1988).
15) Yagi, H. and T. Miyauchi: *Kagaku Kōgaku*, **17**, 382 (1953).